International Journal of Scientific & Engineering Research Volume 9, Issue 5, May-2018
ISSN 2229-5518

Comparative analysis of the maximum power point tracking techniques performance using boost converter

Denis Yamba Sopondja , Bekir Çakır , Mohamed Aboubacar Yasko

Department of Electrical Engineering, Kocaeli University, Kocaeli, Turkey

Email: denilsonyamba1@gmail.com

Abstract *: The efficiency of solar cells depends on many factors such as temperature, insolation, spectral characteristics of sunlight, dirt, shadow, and so on. PV systems use different algorithms to track the maximum power point at any environmental conditions .This article presents the comparative analysis of Constant voltage, perturbation observe and incremental conductance (IncCond) maximum power point tracking (MPPT) methods performance used in solar array power systems using Boost converter .The IncCond ,Perturb and observe algorithm are used to track MPPs because are perform precise control under rapidly changing atmospheric conditions. The Constant voltage is used because is the simplest MPPT control method. ,The controller tracks and feeds maximum power to the load. The linguistic variables have been selected appropriately to modulate the firing angle of the converter for tracking the maximum power. The Simulink model of the proposed scheme employing constant voltage, incremental Conductance and perturbation and observe MPPT controller has been built using MATLAB – SIMULINK. In this work we compare three MPPT techniques performance on the basis of their advantage, disadvantages, control variables involved, types of circuit and complexity of algorithm implementation on MATLAB-SIMULINK.*

Key words : *Incremental conductance (IncCond), constant voltage, incremental conductance, Maximum power point tracking (MPPT), photovoltaic (PV) system, Boost converter.*

I. Introduction

Converting solar energy into electrical energy by PV installations is the most recognized way to use solar energy. Since solar photovoltaic cells are semiconductor devices, they have a lot in common with processing and production techniques of other semiconductor devices such as computers and memory chips. As it is well known, the requirements for purity and quality control of semiconductor devices are quite large. With today's production, which reached a large scale, the whole industry production of solar cells has been developed and, due to low production cost, it is mostly located in the Far East. Photovoltaic cells produced by the majority of today's most large producers are mainly made of crystalline silicon as semiconductor material.

Solar photovoltaic modules, which are a result of combination of photovoltaic cells to increase their power, are highly reliable, durable and low noise devices to produce electricity. The fuel for the photovoltaic cell is free. The sun is the only resource that is required for the operation of PV systems, and its energy is almost inexhaustible.

Recently, energy generated from clean, efficient, and environmentally friendly sources has become one of the major challenges for engineers and scientists. Among all renewable energy sources, solar power systems attract more attention because they provide excellent opportunity to generate electricity while greenhouse emissions are reduced.

Regarding the endless aspect of solar energy, it is worth saying that solar energy is a unique prospective solution for energy crisis. However, despite all the aforementioned advantages of solar power systems, they do not present desirable efficiency. [4,5]

The efficiency of solar cells depends on many factors such as temperature, insolation, spectral characteristics of sunlight, dirt, shadow, and so on. Photovoltaic array (PV) find various applications such as those for the household appliances, for the solar cars, and for the electric aircrafts or space crafts. Changes in insolation on panels due to fast climatic changes such as cloudy weather and increase in ambient temperature can reduce the photovoltaic (PV) array output power. In addressing the poor efficiency of PV systems, some methods are proposed, among which is a new concept called "maximum power point tracking" (MPPT). All MPPT methods follow the same goal which is maximizing the PV array output power by tracking the maximum power on every operating condition.

In the use of solar panels, maximum power point tracking is the automatic adjustment of electrical load to achieve the greatest possible power harvest, during moment to moment variations of light level, shading, temperature, and photovoltaic module characteristics. Solar cells have a complex relationship between solar irradiation, temperature and total resistance that produces a non-linear output efficiency known as the "I-V curve"; it is the purpose of the MPPT system to sample the output of the cells and apply a new MPPT system has been developed using single ended resistance (load) to obtain maximum power for any given environmental conditions.

The converter acts as an interface between the PV module and the load. The controllers are used to track the maximum

power of PV array and control action is taken in such a way that the maximum power is tracked in the PV systems thereby improving the efficiency of the systems.
The are many new MPPT techniques such as distributed MPPT: Perturb and observe, Fractional open circuit voltage, Fractional open short circuit current, incremental conductance, Constant Voltage ...etc. [6,7]

In this work we compare three MPPT techniques on the basis of their advantages, disadvantages, control variables involved, types of circuit and complexity of algorithm implementation on MATLAB-SIMULINK.

In this article the methodology is described in section II. Electric characteristics of photovoltaic cells and Module is presented in section III , Boost Converter in section IV .Maximum Power Point tracking Algorithms, in section V. Design, Modeling and simulation results in section VI and Conclusion in section VII.

II. PROPOSED METHODLOGY

The block diagram of the proposed scheme is shown in Fig.2.1.This scheme of power generation consists of PV system , Boost converter, Constant Voltage/Perturb and observe /incremental conductance. The PV system converts the solar radiation into electrical power. The proposed scheme has been built on a PV system (SUNGEN INT SGM – 200 P) of P=200W;Ppm=199.88W;Vpm=27.8V; Ipm=7.19A; Voc=34.2V;Icc=7.7A. The power is fed to the Boost Converter. Converter and the triggering pulse to the converter is given by the constant voltage, perturb and observe or incremental conductance algorithm. Hence the load is maintained to operate at maximum power.

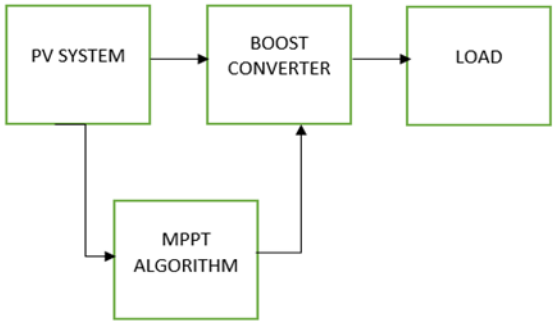

Fig. 2 Block diagram of the proposed methodology

III. Electric characteristics of photovoltaic cells and Module

III.1 Electric characteristics of photovoltaic cells

A PV cell is in fact a well-known electronic component called “LED” (Light Emitting Diode), a component that lets pass the electric current in one direction (with a voltage drop of about 0.6 volt) and that blocks its passage in the other direction. In the case of a PV cell, we try to keep the surface of the junction as wide as possible to collect the maximum of solar energy. The simplified electric diagram of such a PV cell is shown in the following figure 2.

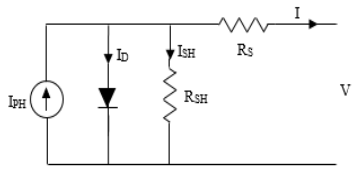

Fig. 3.1 Electrical scheme of a PV cell

One recognizes the symbol of the diode (crossed by the current I_d), in parallel with the generator of current I_{CC}, which corresponds to the flow of electrons generated by the flow of photons from the light (solar or otherwise) within the junction of the diode. Also in parallel to the diode there is the resistance Rsh (shunt resistance), which corresponds to the direct losses through the junction. In series towards the V_P and Ip usage, is the resistance R_S (series resistance) that corresponds, amongst other things, to the Joule losses in the wires. At the two poles of photovoltaic cell, electrical energy is recovered under the form of a voltage V_P and of a current Ip. The equation between Ip and Vp is the following:

$$Ip = Icc - Is\left(e^{\frac{V_P + I_P.R_S}{\frac{KT}{q}}} - 1\right) - \frac{V_P + I_P.R_S}{Rsh} \qquad \text{(III.1)}$$

Where:

I_{CC} = variable generated current according to light radiance
T = temperature in K
K = 1.38 10^{-23}J/K (Boltzmann constant)
q = 1.6 10^{-19} C (electron charge)
Is = some nA (own characteristic of each charge diode)
Rsh = shunt resistance
Rs = series resistance

The layout of the equation IP = f(Vp) looks like on this curve, one can recognize the curve of the diode (to the bottom because of the sign - in the equation) and shifted to the top of the value I_{CC} from the current generated by luminous radiance.
Characteristic Points on this curve for a crystalline silicon cell:

No-load Voltage (I_P = 0 A) Voc = 0.6 V (power P = 0W)
Short-circuit current (Vp=0V) = I_{CC} (variable according to radiance, power P=0W)
Charging Voltage Vpm = 0.5 V at the point of operation where the power is maximum Current Ipm (variable according to radiance) at the point of operation where the power is maximum power: Pmax = Ipm × Vpm

Note that, while varying Vpm from 0 to Voc (or I_P from 0 to I_{CC}), the power starts from 0W to go up to reach Pmax , then to go down again to 0W.

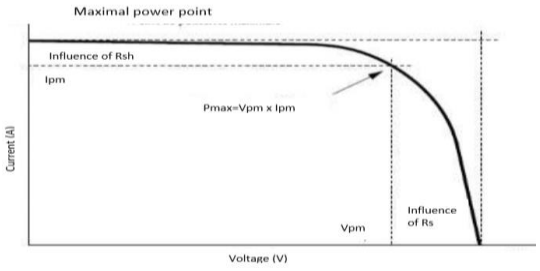

Fig.3.2 Equation Ip =f(Vp)

The output of luminous energy conversion in electrical energy of a photovoltaic cell of surface S, of a Pmax power under a luminous radiance Ir is the following:

$$R_{Cell} = \frac{Pmax(W)/S(m2)}{Ir(\frac{W}{m2})} \qquad \text{(III. 2)}$$

One define also a factor of form (or fill factor), noted FF, representing the quality of a photovoltaic cell:

$$FF = \frac{Vpm\ X\ Ipm}{Voc\ X\ I_{CC}} \qquad \text{(III.3)}$$

III.2 Electric characteristics of photovoltaic module

The voltage of 0.5 V delivered by a photovoltaic cell is much too weak for most implementations. To Increase the voltage, the photovoltaic modules are composed of photovoltaic cells assembled in series to increase the voltage.

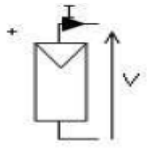

Fig. 3.3 Electric symbol of photovoltaic module

On fig. 3.3 electric symbol of photovoltaic module, historically, the first photovoltaic modules included 36 PV cells in series (0.5 V). They were used in isolated sites to charge the 12 volts lead-acid batteries and, because of that, these modules are known as the 12V type. The voltage of 18 volts makes it possible to charge 12V batteries until fully charged (typically 14.8 volts), even with a weak irradiation (where the voltage slightly drops).

Currently, there is no market for battery chargers since most of the photovoltaic installations in the world are connected to grid, so the number of the cells in series can be higher, in general of 48, 54, 60, 72, 96 cells (standard of 60 cells).
In short, the photovoltaic cells are assembled in series to create photovoltaic modules, then the Modules are assembled in series and in parallel to form photovoltaic field .

The characteristic curve of a photovoltaic module (for various radiances) for the output current and power (i.e. product Voltage-Intensity) according to the output voltage are represented in the following figures for photovoltaic module :

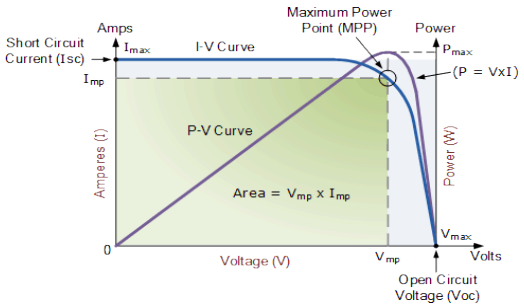

Fig.3.4 Solar I-V characteristic curve [18]

From fig.3.4, the electric characteristics of PV modules are given into one point of operation described under the term of STC (Standard Test Conditions), which are:
- Solar irradiation of 1000 W/m ²
- Solar spectrum AM 1.5
- Temperature of 25°C
- VOC, No-load Voltage (Intensity = 0A) in figure 1.11 (Voc on the curve)
- Short-circuit Intensity ICC (tension = 0V) in figure 1.11 (Icc on the curve)
- Maximum voltage of use at the point of maximum output Vmax in figure 1.11(Vmax on the curve)
- Maximum Intensity of use at the point of maximum output Imax in figure 2.11 (Imax on the curve)
- The point of maximum output, Pmax in figure 1.11 (Pmax on the curve) at the point of function described as STC conditions (1 000 W/m ², spectrum AM1.5 and 25°C), the maximum capacity is the peak power Pc of the photovoltaic module, this peak power is expressed in Watts Peak.

According to the curves plotted above for various radiances (1000, 750 and 400W/m², and a surface cell temperature of 25°C), one notes that the optimum point of operation in power is variable in current and voltage. That means, for the load connected to a module (or a photovoltaic field) to function at this optimum power, the installation will have to include an electronic device that will search for this point of maximum power. This system is called MPPT (for Maximum Power Point Tracking). Typically, inverters include this function.
Relation between surface S (in m²), the output of luminous energy conversion into electrical energy (Rmod) and the peak power of a photovoltaic module (in Wp).

. On the basis of the formula for the output of a cell:

$$\text{Rcell} = \frac{Pmax(W)/S(m2)}{Ir(\frac{W}{m2})} \ , \qquad \text{(III.4)}$$

Already considered, before and by remembering that the power peak Pc is defined under conditions STC, we can write:

Pc(in Wp) = S (en m2) X Rmodule X 1000 W/m2 (III.5)
Pc (in kWp) = S (en m2) X Rmodule X 1KW / m2 (III.6)

Note: the output of a photovoltaic module is generally slightly lower than the output of the cells it is made of, because surface is lost between the cells and it is also necessary to count the surface of the framework. [10,11]

IV. Boost Converter

If the three elements *S*, *L*, and *d* of the buck converter are rearranged as shown in Figure 2.1a, a boost converter is created. Its equivalent circuits during switch-on and switch-off are shown in Figure 2.1b and 2.1c.

IV.1 Voltage Relations

When the switch *S* is on, the inductor current increases:

$$\frac{dI_L}{dt} = \frac{V_1}{L} \qquad \text{(IV.1)}$$

Since the diode is inversely biased, the capacitor supplies current to the load, and the capacitor current *Ic* is negative. Upon opening the switch, the inductor current must decrease so that the current at the end of the cycle can be the same as that at the start of the cycle in the steady state.

For the inductor current to decrease, the value *V*C = *V*2 must be >*V*1. For this interval with the switch open, the inductor current derivative is given by

$$\frac{dI_L}{dt} = \frac{V_1 - Vc}{L} = \frac{V_1 - V2}{L} \qquad \text{(IV.2)}$$

A graph of the inductor current versus time is shown in Fig. 4.2

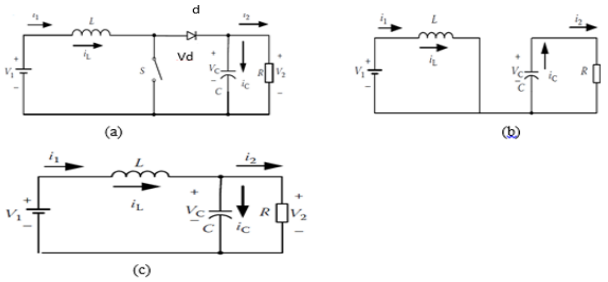

Fig.4.1 Boost converter: (a) circuit, (b) switch-on, and (c) switch-off

$$Imax - Imin = \frac{V1}{L} DT \qquad \text{(IV.3) And}$$

$$Imin - Imax = \frac{V_1 - V_C}{L}(1 - D)T; \qquad \text{(IV.4)}$$

$$V_2 = V_C = \frac{V_1}{1-D} \qquad , \qquad \text{(IV.5)}$$

Fact, as D approaches unity, the output voltage decreases rather than increasing because of the effect of circuit parasitic elements. The value of D must be limited within a certain upper limit (say 0.9) to prevent such a problem. Practical limits to this also become important for an increase in the voltage transfer gain, for example, The switch may be open for only a very short time (0.1 *T* since D = 0.9). [29]

IV.3 Circuit Currents

The Imax and Imin values can be found via the input average power and the load average power, if there are no power losses:

$$Pin = \frac{\text{Imax} - \text{Imin}}{2} V_1 \qquad \textit{(}\text{input power}\textit{)} \qquad \text{(IV.6)}$$

$$Po = \frac{V_2{}^2}{R} \qquad \textit{(}\text{output power}\textit{)}. \qquad \text{(IV.7)}$$

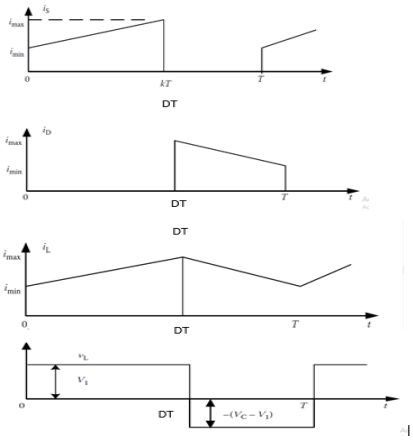

Fig. 4. 2 Some current and voltage waveforms.

Considering Equation IV.5, we have

$$Imax - Imin = 2\frac{\text{V1}}{R(1-D)^2} \qquad \text{(IV.8)}$$

From Equations IV.4 and IV.8

$$Imin = \frac{\text{V1}}{R(1-D)^2} - \frac{\text{V1}}{2L}\,\text{DT}, \qquad \text{(IV.9)}$$

$$Imax = \frac{\text{V1}}{R(1-D)^2} + \frac{\text{V1}}{2L}\,\text{DT}\,. \qquad \text{(IV.10)}$$

The load current value I_2 is given by $I_2 = \frac{V2}{R}$, and the average current flowing through the capacitor is zero. The instantaneous capacitor current is likely a triangular waveform, which is approximately ($I_L - I_2$) during switch-off and $-I_2$ during switch-on. From Figure 2.1, the input source current $I_1 = I_L = I_S$ continuous. Hence, the buck converter operates in CICM.

IV.4 Continuous Current Condition

When the Imin is equal to zero, the minimum inductance can be determined to ensure a continuous inductor current. Using Equation IV.9 and solving it, we obtain

$$Lmin = \frac{D(1-D)^2}{2}\,\text{TR} \qquad \text{(IV.11)}$$

The change of the charge across the capacitor *C* is

$$\Delta Q = DTI_2 = DT\frac{V_2}{R}\,\text{TR} = \frac{\text{DTV}_1}{(1-D)R} \qquad \text{(IV.12)}$$

Therefore, the ripple voltage ΔV_C across the capacitor *C* is

$$\Delta V_C = \frac{\Delta Q}{C} = \frac{\text{DTV}_2}{RC} = \frac{\text{DTV}_1}{(1-D)RC} \qquad \text{(IV.13)} \quad [29]$$

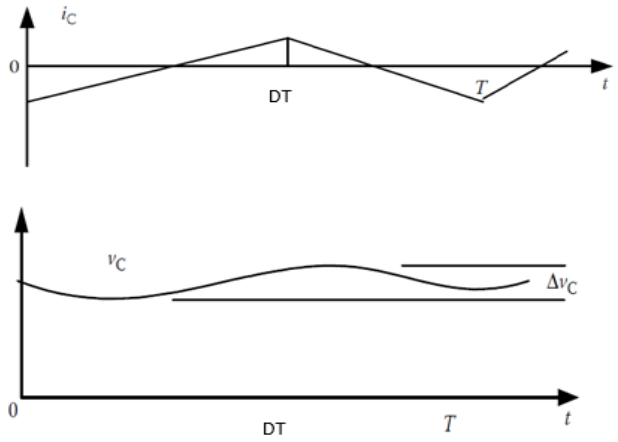

Figure 4.3 Waveforms of I_C and V_C.

V .PROPOSED ALGORITHMS

There are many new MPPT techniques algorithm but as part of our work, we approach some, such as:

V.1 Fractional open circuit voltage

The open-circuit technique is based on the fact that the ratio of PV array output voltage *VMPP* at the maximum power point to its open circuit voltage *Voc* is approximately constant under varying irradiation and temperature levels as shown in the Equation (V.1) [19, 20, 21].

$$VMPP \approx Kv\, Voc \qquad (V.1)$$

Kv is the proportional constant which depends on the characteristic of the photovoltaic array being used. Therefore it has to be estimated by empirically determining *Voc* and *VMPP* for the particular PV array at different levels of temperature and irradiation. However the value of *Kv* has been reported to range between 71% and 80%. Fig. 3.1 shows the fractional open circuit voltage algorithm flowchart. The open circuit voltage *Voc* is measured by momentarily interrupting the normal operation of the system.

This is done by introducing a static switch in series with the PV array. Once *Kv* is known and *Voc* is measured, the *VMPP* value can be calculated from Equation (V.1) as a reference and a feed forward voltage control scheme is implemented to bring the PV array voltage to the point of peak power.

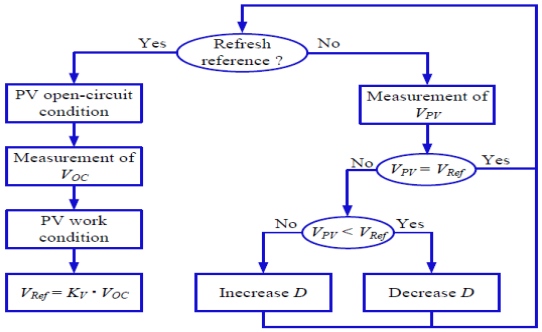

Fig. 5.1 Fractional short circuit voltage

This method has an advantage that it is very simple, cheap to implement and it uses only one feedback loop. However, its drawback is that the interrupted system operation at the time of measuring *Voc* results in some generated power loss.

To prevent this, the authors in [24, 25] used pilot cells to obtain *Voc*. The pilot cells are solar cells that represent the PV array's cells, which are not used to produce electricity but to obtain the characteristic parameters such as *VOC* without interrupting the main PV system. The pilot cells must be carefully chosen to represent the characteristics of photovoltaic array. Hence, each pair of pilot cell/solar array must be calibrated, consequently, increasing the energy cost of the system.

V.2 Fractional Short Circuit Current method (FSCC)

The basis for short-circuit current method is that, the maximum operating current *IMPP* is approximately linearly related to the short-circuit current *Isc* under varying atmospheric conditions; in other words:

IMPP ≈ *Ksc* . Ioc (V.2)

Where *Ksc* is a proportional constant and it depends mainly on the metrological conditions and fill factor. The proportional constant *Ksc* is usually found to be between (75% - 92%) . The algorithm flowchart of the fractional short-circuit current is shown in Fig. 5.2. To measure Isc an additional switch has to be introduced in parallel with the PV array to satisfy the short circuit condition. However the author in [26] provided another option by using a boost converter and the switch of the converter is used for short circuiting the PV array. Once Ksc is known and Isc is measured the IMPP can be calculated from Equation (V.2).

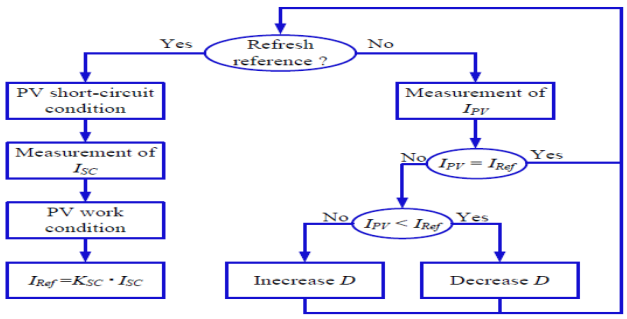

Fig. 5.2 FSCC algorithm

The advantages of this method are its simplicity and low cost of implementation. On the other hand, the momentary interruption required for measuring *ISC* leads to some loss of generated power, and the value of *Ksc* changes slightly [27, 28].

V.3 PERTURB AND OBSERVE (P&O)

P&O is one of the most discussed and used algorithms for MPPT. The algorithm involves introducing a Perturbation in the panel operating voltage. Modifying the panel voltage is done by modifying the converter duty cycle. The way this is done becomes important for some converter topologies. Looking at Figure 5.3 makes it easy to understand that decreasing voltage on the right side of the MPP increases power. Also, increasing voltage on the left side of the MPP increases power. This is the main idea behind P&O. Let's say that, after performing an increase in the panel operating voltage, the algorithm compares the current power reading with the previous one. If the power has increased, it keeps the same direction (increase voltage), otherwise it changes direction (decrease voltage). This process is repeated at each MPP tracking step until the MPP is reached. After reaching the MPP, the algorithm naturally oscillates around the correct value.

The basic algorithm uses a fixed step to increase or decrease voltage. The size of the step determines the size of the deviation while oscillating about the MPP. Having a smaller step will help reduce the oscillation, but will slow down tracking, while having a bigger step will help reach MPP faster, but will increase power loss when it oscillates.
To be able to implement P&O MPPT, the application needs to measure the panel voltage and current. While implementations that use only one sensor exist, they take advantage of certain hardware specifics, so a general purpose implementation will still need two sensors.

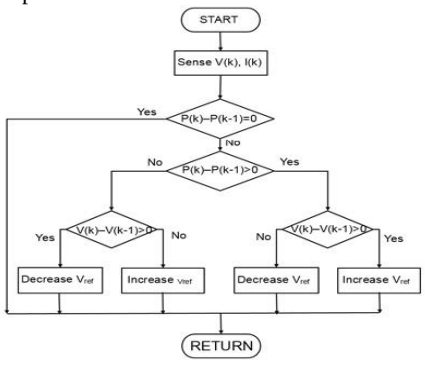

Fig. 5.3 PO algorithm

V.4 INCREMENTAL CONDUCTANCE

The incremental conductance algorithm uses the fact that the panel power curve derivative (or slope) versus voltage is 0 at MPP, positive on the left side and negative on the right side of the MPP.

$\frac{dP}{dV} = 0\ , at\ MPP$ (V.3)

$\frac{dP}{dV} > 0\ ,\ Left\ at\ MPP$ (V.4)

$\frac{dP}{dV} < 0\ , Right\ at\ MPP$ (V.5)

The power derivative can be also written as:

$\frac{dP}{dV} = \frac{d(VI)}{dV} = I\frac{dV}{dV} + V\frac{dI}{dV} = I + V\frac{dI}{dV} \cong$ I+ V$\frac{\Delta I}{\Delta V}$ (V.6)

$\frac{\Delta I}{\Delta V} =$ - $\frac{I}{V}$, at MPP (V.7)

$\frac{\Delta I}{\Delta V} >$ - $\frac{I}{V}$, at Left MPP (V.8)

$\frac{\Delta I}{\Delta V} <$ - $\frac{I}{V}$, at Right MPP (V.9)

The main idea is to compare the incremental conductance ($\frac{\Delta I}{\Delta V}$) to the instantaneous conductance ($\frac{I}{V}$). Depending on the result, the panel operating voltage is either increased, or decreased until the MPP is reached. Unlike the P&O algorithm, which naturally oscillates around the MPP, incremental conductance stops modifying the operating voltage when the correct value is reached. A change in the panel current will restart the MPP tracking. Depending on the ambient conditions, the same functionality may be achieved by using the initial equation ($\frac{\Delta I}{\Delta V}$).
The basic incremental conductance algorithm uses a fixed step size for the panel operating voltage updates. Using a bigger step size will speed up tracking, but may also cause the algorithm to oscillate around the MPP instead of locking on. Implementing the incremental conductance algorithm requires the voltage and the current output values from the panel (two sensors). Because it needs to keep track of previous voltage and current values, this algorithm is usually implemented using a PIC® device or a DSP.

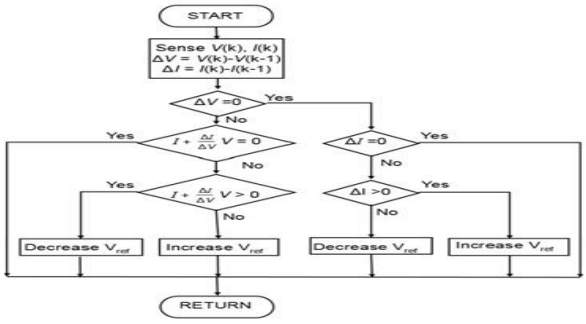

Fig. 5.4 Incremental conductance algorithm

V.5 Constant Voltage method (CV)

The constant voltage tracking algorithm is the simplest MPPT control method. The feedback of the PV voltage is compared with a fixed reference voltage (*Vref*) and the resultant signal adjusts the duty ratio of the DC-DC converter to keep the operating point of the PV array near the MPP. The reference voltage value is set to be equal to the maximum voltage of the characteristic PV module or to another calculated best fixed voltage. In this method, the maximum power point occurs between 72% and 78% of the open circuit voltage, for the standard atmospheric condition [22]. The duty ratio (D) of the DC-DC converter ensures that the PV voltage is equal to:

$$V\text{ref}=\text{Kc}V\text{oc} \qquad (V.10)$$

Where *K*c = 0.72-0.78 and *Vref* which is calculated and kept constant during one sampling period by hold circuit in order to make duty ratio adjusting *V*pv= *V*ref. For next sample again *V*oc is sampled and the same procedure is repeated for each sample.

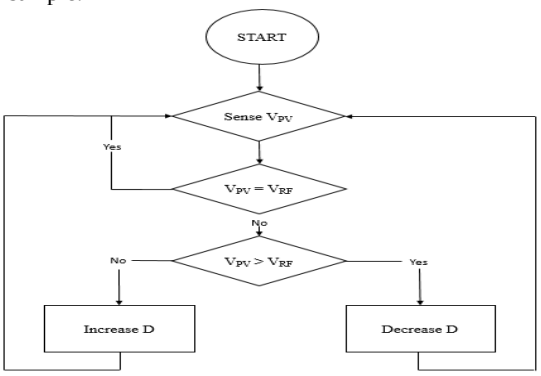

Fig. 5.5 CV algorithm

This method is simple, economical and only one feedback-loop control is required. However this technique has the drawback that it assumes that individual insulation and temperature variations on the array are insignificant and the constant reference voltage is an adequate approximation of the true MPP [23].

VI .Design, Modeling and simulation results

VI.1 Design of Boost converter

VI.1.1 Electrical characteristics of PV photovoltaic

Electrical characteristics data of PV module and cells of SUNGEN INT SGM – 200 P	values
Electric characteristic of module	
Rated Power Pc	200 W
Maximum power(Ppm)	199.882 W
Maximum Power Voltage (*Vpm*)	27.8 V
Maximum Power Current (*Ipm*)	7.19A
Open-Circuit Voltage (*Voc*)	34.2 V
Short-Circuit Current (*Isc*)	7.77 A
Temperature Coefficient (*Voc*)	-0.36044 V / °C
Temperature Coefficient (*Isc*)	0.052819 A / °C
Electric characteristics of cells	
Light-generated IL(A)	7.8256 A
Diode saturation I0(A)	2.6241e-10 A
Diode ideality factor	0.92138
Shunt resistance Rsh (Ohms)	111.3843 Ohms
Series resistance (Ohms)	0.30346 Ohms
Number of cells (N)	60

Table 6.1: electric Characteristic of PV module SUNGEN INT SGM – 200 P

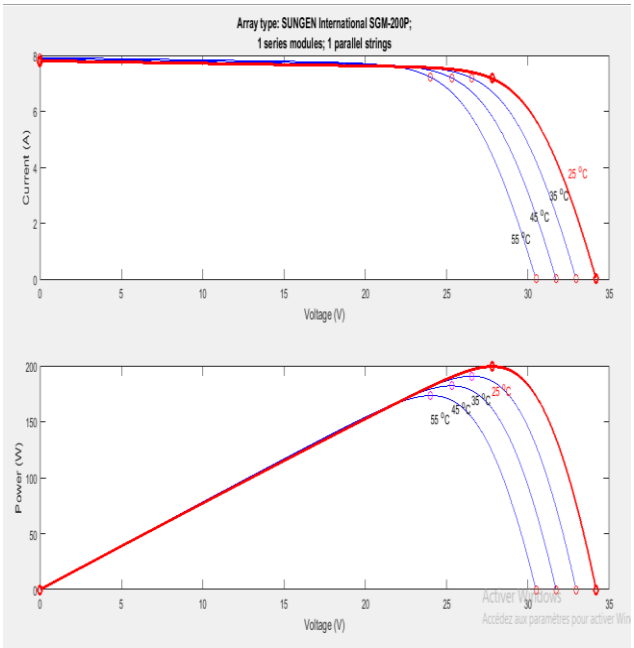

Fig.6.1 I-V characteristics of SUNGEN INTERNATIONAL SGM-200P

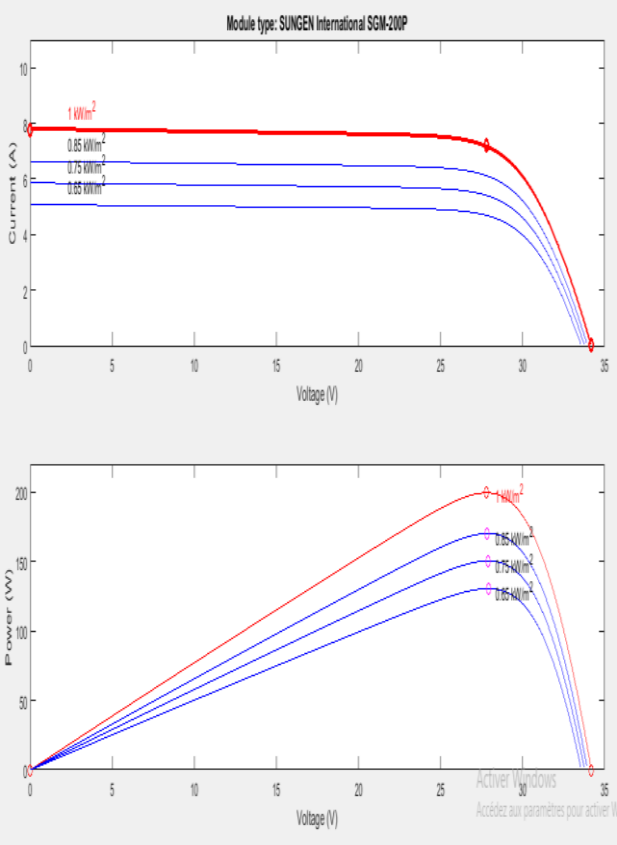

Fig.6.2 I-V characteristics of SUNGEN INTERNATIONAL SGM-200P

Test conditions $\frac{W}{m^2}$ / °C	P_{PVmax}	V_{PVmax}
1000/25	199.9	27.8
1000/35	190.8	27.76
1000/45	182.1	27.73
1000/55	173.3	27.69
850/25	170.1	27.49
850/35	170.09	26.5
850/45	170.086	25.54
850/55	170.085	24.62
750/25	150.3	27.24
750/35	150.297	26.26
750/45	150.294	25.31
750/55	150.291	24.40
650/25	130.4	26.96
650/35	130.397	25.98
650/45	130.394	25.04
650/55	130.391	25.13

Table 6.2 The available maximal Power and voltage values of SUNGEN INTERNATIONAL SGM-200P Module photovoltaic

VI.1.2 Design of Boost converter

Boost Converter Parameters	
Vin= V1(V)	27.8
Vout =V2(V)	48
Iin =I1(A)	7.19
Iout=I2(A)	4.164
ΔV	ΔV =1%Vout
ΔI	ΔI =1%Iout
fsh(KHZ)	20

Table 6.3 Boost Converter Parameters

The input capacitor is used to reduce the converter input voltage ripple and determines the amount of peak current drawn from the source. The input capacitor can be calculated Equation (IV.5) with maximum voltage ripple of 1% V2. From the equation (IV.5)

$V_2 = \frac{1}{1-D} V_1 \Rightarrow 1 - D = \frac{V1}{V2} = \frac{27.8}{48} = 0.57916 \Rightarrow D = 0.42083$,From Table 6.3 $\Delta V = 1\%$ V2 ,From the equation (IV.7) ;

$P_2 = \frac{V_2^2}{R} \Rightarrow R = \frac{V_2^2}{P_2} \Rightarrow R = \frac{(48)^2}{199.882} = 11.5268$ Ohms

$P2 = \frac{(V2)^2}{R} \Rightarrow R = \frac{(V2)^2}{P} = \frac{(48)^2}{199.882} = 11.5268$ ohms .

From equation (IV.11) and table 6.3

Lmin $= \frac{(1-D)^2}{2f}$ DR= $\frac{(1-0.42083)^2}{2.20000}$ .0.42084. (11.5268) = 0.0000407 H , or Lmin = 40.7 µH ,From equation (IV.11)

$\Delta V = \frac{\Delta Q}{C} = \frac{DV2}{RCf} = \frac{DV1}{(1-D)RCf}$ *and* $\Delta V = 1\%\ V2 = 0.01V2$

$\Rightarrow \Delta V = 1\%\ V2 = \frac{DV2}{RCf} = 0.01V2 \Rightarrow D = \frac{V2}{RCf}$

⇨ $C_{out} = \frac{DV2}{0.01V2Rf} = \frac{D}{0.01*Rf} = \frac{0.42083}{0.01*11.5268*20000} = 0.000182184$

⇨ H

⇨ or C_{out} = 182.184 µH

⇨ Anotherwise

⇨ Cin $\geq \frac{(1-D)\ I_{PV}\ D}{0.01*Ipvm*Rpvm*Rf}$ and Ipvm ∗ Rpvm = Vmp

⇨ Cin $\geq \frac{(1-D)IpvD}{0.01*Ipvm*Rpvm*Rf}$ anotherwise $I_{pv} = \frac{P_{pv}}{Vmp} = \frac{199.882}{27.8} = 7.19$ A

⇨ => Cin $\geq \frac{(1-0.42)*7.19*0.42}{0.01*27.8*20000} \geq$ 0.000315015 F or Cin ≥ 315 µF

VI.2 Modeling , Simulation results

VI.2.1 PV photovoltaic system connected to Boost Converter

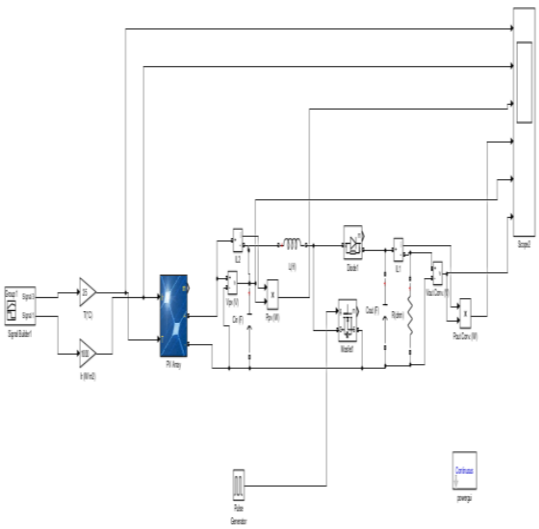

Fig. 6.3 sheme of PV photovoltaic system connected to Boost converter .

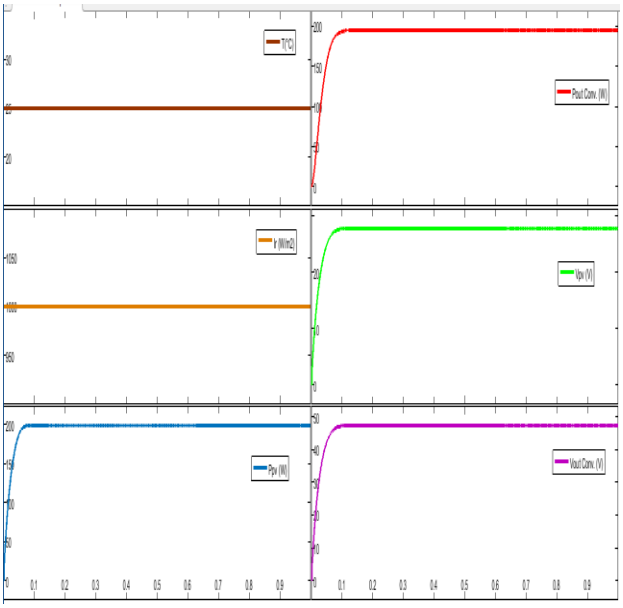

Fig. 6.4 Result of Simulation of the PV Photovoltaic system connected to Boost converter (1000 $\frac{W}{m^2}$, 25 °C)

VI.2.2 PV photovoltaic system connected to Boost controlled by MPPT Perturbation and Observe algorithm

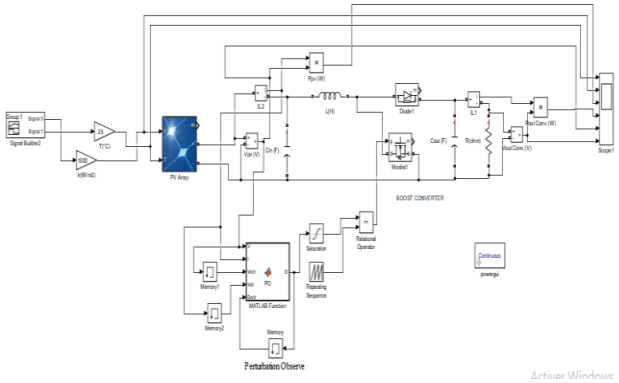

Fig. 6.5: scheme of PV photovoltaic system connected to Boost controlled by MPPT perturbation and observe algorithm

Coding of Perturbation and Observe

```
Function D = PO (  V, I,V old, Iold  ,Dold)
P=V*I;
Pold = Vold*Iold;
dV=V-Vold;
dP=P-Pold;
deltaD= 0.00001;
Di=0.42083;
if dP/dV<0
   D=Di+deltaD;
```

```
else
   D=Di-deltaD;
   if dP/dV>0
      D=Di-deltaD;
   else
      D=Di+deltaD;
   end
   if dP/dV== 0
      D=Dold;
   end
end
```

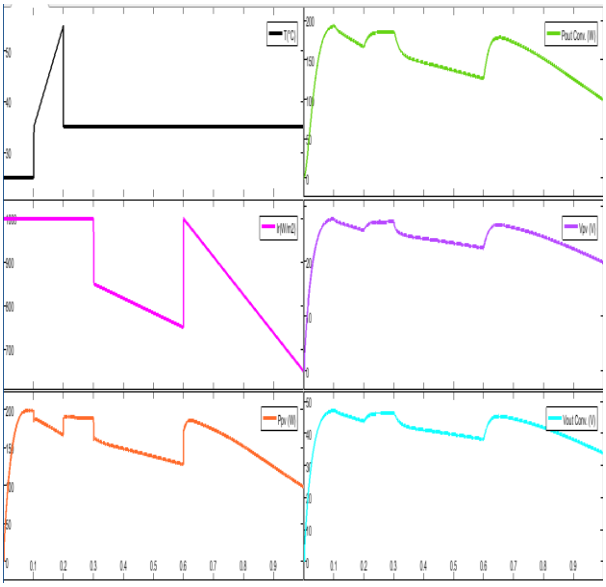

Fig.6.6 Result of simulation of photovoltaic system connected to Boost controlled by MPPT Observe and perturbation algorithm for different values irradiance and temperature

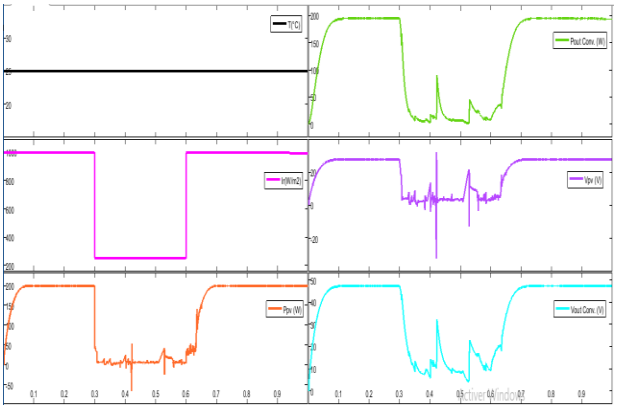

Fig. 6.7 result of simulation of PV photovoltaic system connected to Boost controlled by MPPT perturbation and Observe algorithm for different values irradiance and temperature

Test Conditions W/m² / °C	$P_{PVout(W)}$	$P_{PVout(W)}$	$P_{PVout(}$	P_{PVmax}	η
	ΔD	ΔD	ΔD		
	0.001	0.0001	0.000 01		
1000/25	199.4	199.4	199.4	199.9	99.7%
1000/35	189.8	189.9	189.9	190.8	99.5%
1000/45	178.9	179.1	179.1	182.1	98.3%
1000/55	167.1	167.5	167.6	173.3	96.7%
850/25	159.5	159.5	159.9	170.1	94 %
850/35	157.9	158	158.3	170.09	93%
850/45	150.6	154.2	154.2	170.086	90.6
850/55	147.8	147.9	147.9	170.085	86.9%
750/25	126.6	126.7	126.9	150.3	84.4%
750/35	127.4	127.4	127.7	150.297	84.9%
750/45	127.5	127.5	127.8	150.294	85%
750/55	125.9	126	126.9	150.291	84.4%
650/25	96.13	96.13	96.38	130.4	73.9%
650/35	94.6	97.07	97.4	130.397	74.7%
650/45	97.91	97.91	98.16	130.394	75.3%
650/55	98.44	98.44	98.68	130.391	75.7%

Table 6.4 the power and voltage values of simulation photovoltaic system connected to Boost controlled by MPPT perturbation and Observe algorithm

VI.2.3 Photovoltaic connected to Boost controlled by MPPT Constant Voltage (CV) Algorithm

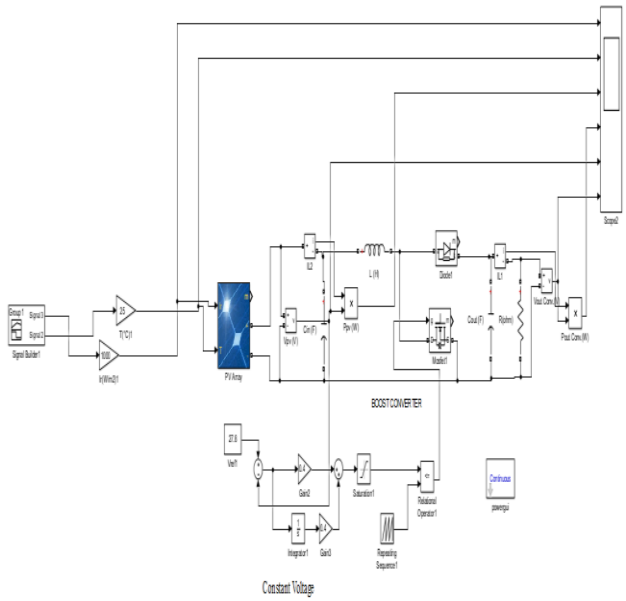

Fig.6.8 scheme of PV photovoltaic system connected to Boost controlled by MPPT CV algorithm

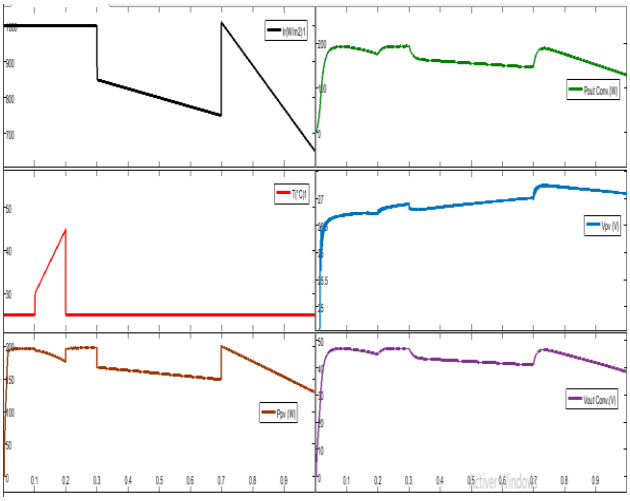

Fig.6.9 Result of simulation of photovoltaic system connected to Boost controlled by MPPT CV algorithm for different values of irradiance and temperature

Test Conditions W/m^2 / °C	$P_{PVout(W)}$	$P_{PVout(W)}$	$P_{PVout(W)}$	P_{PVmax}	η
	ΔD	ΔD	ΔD		
	0.2	0.4	0.6		
1000/25	197.5	199.2	198.9	199.9	99.6 %
1000/35	189.1	190.6	190.1	190.8	99.9 %
1000/45	170.2	180.1	173.6	182.1	98.9 %
1000/55	140.4	161.7	147.7	173.3	93.3 %
850/25	165	169.4	168.6	170.1	99.6 %
850/35	161.9	162.6	162.1	170.09	95.6 %
850/45	146.4	154.7	149.7	170.086	90.9 %
850/55	120.7	140.7	127.8	170.085	82.7 %
750/25	144.8	149.6	148.6	150.3	99.5 %
750/35	142.7	143.8	143.3	150.297	95.7 %
750/45	129.9	137.1	133	150.294	91.2%
750/55	107.1	125.8	113.9	150.291	83.7%
650/25	124.2	129.5	128.4	130.4	99.3%
650/35	123.8	124.7	124.2	130.397	95.6%
650/45	112.4	118.8	115	130.394	91.1%
650/55	93.09	108.7	97.72	130.391	83.4%

Table 6.4 the power and voltage values of simulation photovoltaic system connected to Boost controlled by MPPT CV algorithm for different values of irradiance, temperature and Gain

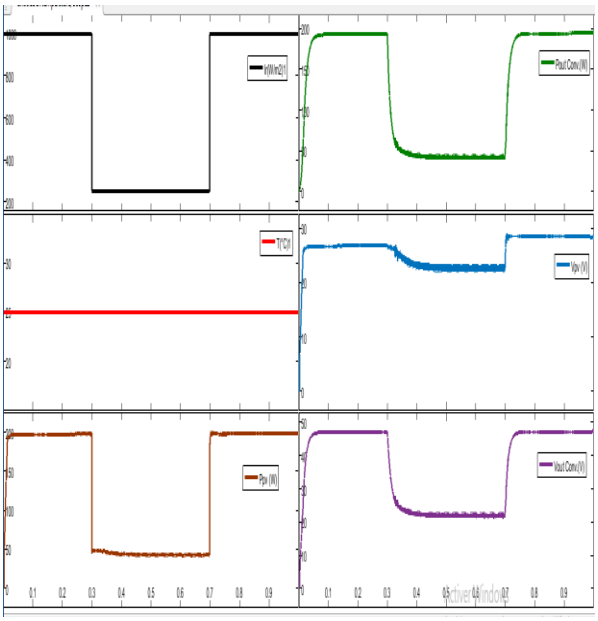

Fig.6.10 Result of simulation of photovoltaic system connected to Boost controlled by MPPT CV algorithm for different values irradiance and temperature.

VI.2.4. Photovoltaic connected to Boost controlled by MPPT Incremental Conductance (Inc)

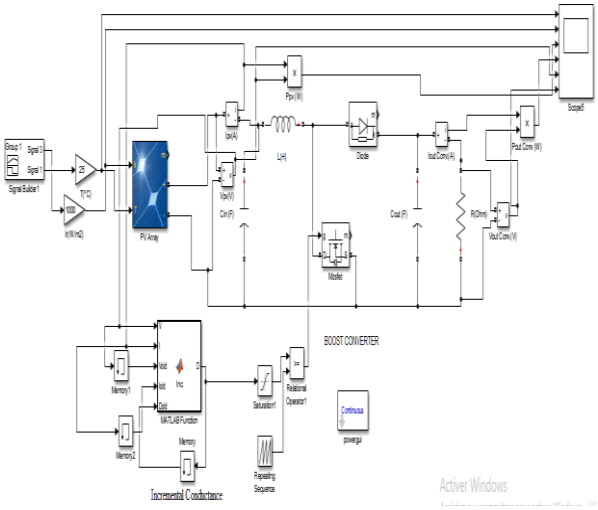

Fig.6.11 sheme of PV photovoltaic system connected to Boost controlled by MPPT Incremental conductance algorithm

Coding of Incremental Conductance

Function D = Inc. (V, I, Vold, Iold, Dold)

dV=V-Vold;

dI=I - Iold;

dD=0.001;

Di=0.42083;

dV=V-Vold

dI=I-Iold;

if dV==0

if dI==0

D=Dold;

else

if dI >0
D=Di+dD;
else
D=Di-dD;
end
end
else
if dI/dV= = -I/V
D=Dold;
else
if dI/dV > - I/V
D=Di – dD ;
else

D=Di+dD;

end

end
end

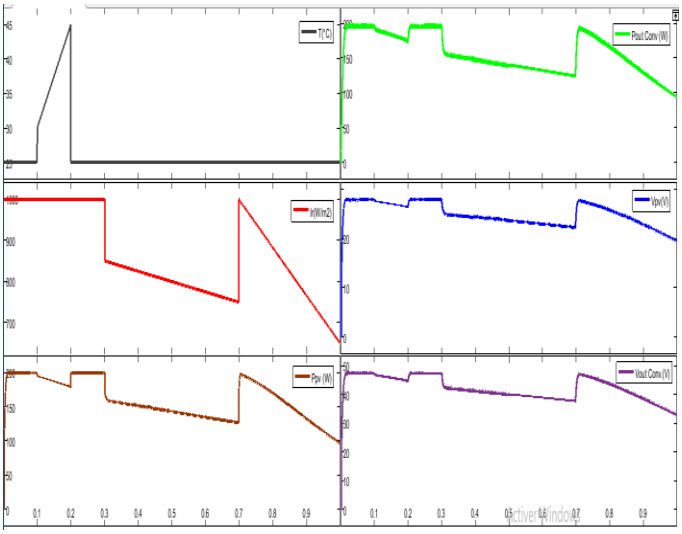

Fig.6.12 : the power and voltage values of simulation photovoltaic system connected to Boost controlled by MPPT Incremental conductance algorithm for different values of irradiance and temperature

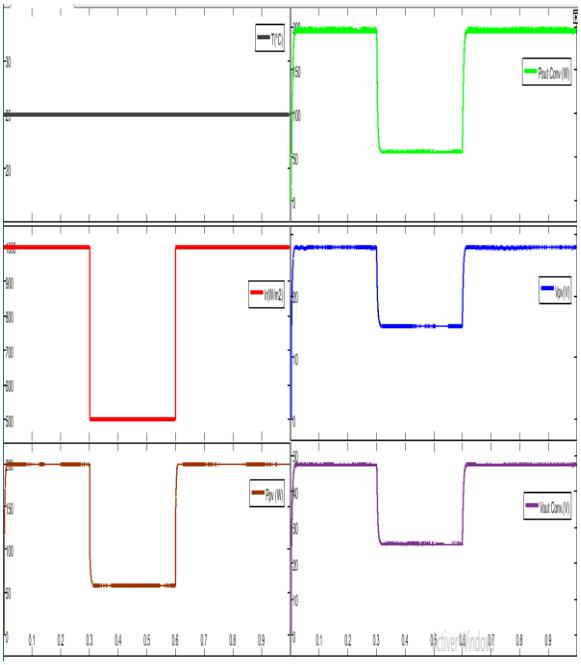

Fig.6.13 the power and voltage values of simulation photovoltaic system connected to Boost controlled by MPPT Incremental conductance algorithm for different values of irradiance and temperature

Test conditions $\frac{W}{m^2}$ / °C	$P_{PVout(W)}$	$P_{PVout(W)}$	$P_{PVout(W)}$	P_{PVmax}	**η**
	ΔD	ΔD	ΔD		
	0.001	0.0001	0.00001		
1000/25	199.6	199.6	199.6	199.9	99.8%
1000/35	190	190.1	190.1	190.8	99.8%
1000/45	179.1	179.3	179.3	182.1	98.4
1000/55	167.6	167.8	167.9	173.3	96.8
850/25	159.3	159.4	159.7	170.1	93%
850/35	158	158	158.3	170.09	93%
850/45	154.1	154.2	154.3	170.086	90.7%
850/55	147.9	147.9	148	170.085	87%
750/25	126.5	126.5	126.6	150.3	84.2%
750/35	125.3	125.4	125.7	150.297	83.6%
750/45	124.1	124.4	124.7	150.294	82.9%
750/55	123	123	123.2	150.291	81.9%
650/25	96.05	96.07	96.31	130.4	73.8%
650/35	95	95.02	95.26	130.397	73%
650/45	93.84	93.86	94.1	130.394	72.1%
650/55	91.39	91.4	92.64	130.391	71%

Table 6.5 the power and voltage values of simulation photovoltaic system connected to Boost controlled by MPPT incremental conductance algorithm for different values of irradiance, temperature.

VII. Conclusion

In this article, it was a question of a comparative analysis of the performance of technical MPPTs for different climatic conditions (temperature, irradiance) by varying the different control parameters (perturbation rate, gain, etc.).

For the Incremental conductance algorithm, three perturbation rate values (0.001, 0.0001, 0.00001) were taken. And it was found that the power was reached when the perturbation rate was equal to 0.00001. For Perturbation and Observe algorithm, it was also taken three perturbation rate values (0.001, 0.0001, and 0.00001). And it was found that maximum power was reached when the perturbation rate was equal to 0.00001. For the constant Voltage algorithm, three gain values (0.2, 0.4, 0.6) were taken and it was found that the maximum power was reached when the gain was equal to 0.4.

In comparison, it has been found that perturb and Observe is more efficient than constant voltage and incremental conductance , it performs precise control in rapidly changing atmospheric conditions ; unfortunately it does not adapt for low irradiance values . Constant voltage and incremental conductance are almost identical; unfortunately are less efficient for low irradiance values.

References

1. R.-J. Wai, W.-H. Wang and C.-Y. Lin, ―High-performance stand-alone Photovoltaic generation system,‖ IEEE Trans. Ind. Electron., vol. 55, no. 1, pp. 240–250, Jan. 2008.
2. N. Mutoh and T. Inoue, ―A control method to charge series-connected ultra electric double-layer capacitors suitable for photovoltaic generation systems combining MPPT control method,‖ IEEE Trans. Ind. Electron., vol. 54, no. 1, pp. 374–383, Feb. 2007.
3. R. Faranda, S. Leva, and V. Maugeri, MPPT Techniques for PV Systems: Energetic and Cost Comparison. Milano, Italy: Elect. Eng. Dept. Politecnicodi Milano, 2008, pp. 1–6.
4. Z. Yan, L. Fei, Y. Jinjun, and D. Shanxu, ―Study on realizing MPPT by improved incremental conductance method with variable step-size,‖ in Proc. IEEE ICIEA, Jun. 2008, pp. 547–550.
5. F. Liu, S. Duan, F. Liu, B. Liu, and Y. Kang, ―A variable step size INC MPPT method for PV systems, IEEE Trans. Ind. Electron., vol. 55, no. 7, pp. 2622–2628, Jul. 2008.
6. https://www.nrel.gov/pv/assets/images/efficiency-chart.png
7. Muhammad H. Rashid, Power Electronics Handbook: Devices, Circuits, and Applications Third Edition, 2011, Elsevier Inc, page 249-257
8. Stuart R Wenham (Editor), Martin A Green (Editor), Muriel E Watt (Editor), Richard Corkish (Editor), "Applied Photovoltaics", Routledge, 2013.
9. Dezso Sera , Laszlo Mathe , Tamas Kerekes, Sergiu Viorel Spataru On the Perturb-and-Observe and Incremental Conductance MPPT Methods for PV Systems Article in IEEE Journal of Photovoltaics • July 2013
10. Rijeka (editor) ‘’Photovotaic systems ‘’ january 2012
11. EREC, Renewable energy in europe, 2010.
12. N. Femia, G. Petrone, G. Spagnuolo, and M. Vitelli, “Optimization of Perturb and Observe maximum power point tracking method,” IEEE T. Power. Electr., vol. 20, no. 4, pp. 963–973, 2005.
13. Fang Lin Luo , Hong Ye, Power electronics : advanced conversion technologies pp. 139-150, taylor 2010
14. Les convertisseurs de l’electronique de puissance Vol.4 ;1989
15. Electronique appliquée , electromecanique sous simscape et SimPowersystems (matlab/simulink) , Mohand Mokhtari Nadia Martaj ,2012
16. http://www.mpptsolar.com/en/solar-panels-in-parallel.html
17. http://www.alternative-energy-tutorials.com/energy-articles/connecting-solar-panels-together.html
18. http://www.alternative-energy-tutorials.com/energy-articles/solar-cell-i-v-characteristic.html
19. J. Ahmad, "A fractional open circuit voltage based maximum power point tracker for photovoltaic arrays," in Software Technology and Engineering (ICSTE), 2010 2nd International Conference on, 2010, pp. V1-247-V1-250.
20. M. A. S. Masoum, et al., "Theoretical and experimental analyses of photovoltaic systems with voltageand current-based maximum power-point tracking," Energy Conversion, IEEE Transactions on, vol. 17, pp. 514-522, 2002.
21 M. A. S. Masoum and H. Dehbonei, "Design, construction and testing of a voltage-based maximum power point tracker (VMPPT) for small satellite power supply," 1999.

22. D. Verma, S. Nema, A.M. Shandilya, S.K. Dash, Maximum power point tracking (MPPT) techniques: Recapitulation in solar photovoltaic systems, Renewable and Sustainable Energy Reviews 54(2016) 1018–1034.

23. R. Faranda, S. Leva, Energy comparison of MPPT techniques for PV Systems, WSEAS Transactions on Power Systems, Issue 6, Volume 3, June 2008 446-455.

24. G. W. Hart, *et al.*, "Experimental tests of open-loop maximum-power-point tracking techniques for photovoltaic arrays," *Solar Cells*, vol. 13, pp. 185-195, 1984.

25. Z. M. Salameh, *et al.*, "Step-down maximum power point tracker for photovoltaic systems," *Solar Energy*, vol. 46, pp. 279-282, 1991.

26. S. Yuvarajan and X. Shanguang, "Photo-voltaic power converter with a simple maximum-power-point-tracker," in *Circuits and Systems, 2003. ISCAS '03. Proceedings of the 2003 International Symposium on*, 2003, pp. III-399-III-402 vol.3.

27. T. Noguchi, *et al.*, "Short-current pulse-based maximum-power-point tracking method for multiple photovoltaic-and-converter module system," *Industrial Electronics, IEEE Transactions on*, vol. 49, pp. 217-223, 2002.

28. M. Abou El Ela and J. A. Roger, "Optimization of the function of a photovoltaic array using a feedback control system," *Solar Cells*, vol. 13, pp. 107-119, 1984.

29. Fang Lin Luo , Hong Ye , " Power Electronics (Advanced Conversion Technologies)" ,pp146-149 ,2010.

.